Inorganic Chemistry

pubs.acs.org/IC

Article

Self-Assembly of Multinuclear Sandwich Silver(I) Complexes by Cooperation of Hexakis(azaheteroaryl)benzene Ligands, Argentophilic Interactions, and Fluoride Inclusion

Miha Drev, Uroš Grošelj, Drago Kočar, Franc Perdih, Jurij Svete, Bogdan Štefane, and Franc Požgan*

Cite This: *Inorg. Chem.* 2020, 59, 3993−4001

Read Online

ACCESS | Metrics & More | Article Recommendations | Supporting Information

ABSTRACT: Self-assembly of AgOTf and AgF with the hexatopic ligands hexakis(pyridin-2-yl)benzene (**2**) and 2,4,6-tris(pyridin-2-yl)-1,3,5-tris(quinolin-2-yl)benzene (**3**) affords the discrete sandwich-shaped complexes $[Ag_4F(\mathbf{2})_2](OTf)_3$, $[Ag_4F(\mathbf{3})_2](OTf)_3$, and $[Ag_5F(\mathbf{2})_2](OTf)_4$. The solid-state structures of the complexes were characterized by single-crystal X-ray diffraction analysis, which revealed that the fluoride anion is coordinated in the center of the Ag_4-square or Ag_5-pentagon units which are positioned between two molecules of the hexakis(azaheteroaryl)-benzene. The generation of complexes is dictated by a unique cooperation of ligand coordination, argentophilicity, and fluoride anion inclusion. All three complexes adopt highly symmetrical structures in solution, as evidenced by appearance of one set of proton resonances for the two ligands arranged face to face.

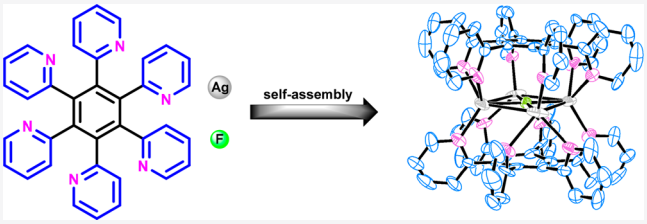

INTRODUCTION

Self-organization of organic molecules, playing the role of ligands, by metal coordination to generate supramolecular architectures of different shapes and sizes is an intensely attractive area in supramolecular chemistry.[1] In the context of ligand design, pyridine derivatives exhibit high stability and tolerance to fluctuating redox environments and have been ubiquitously employed for the construction of metallosupramolecular entities,[2] as well as in crucial catalytic transformations, as Ir^{III}(2-phenylpyridinato)$_3$ and $[Ru^{II}$(2,2′-bipyridine$)_3]^{2+}$ complexes[3,4] are known to be efficient photoredox systems.[5] Examples of multinuclear Ag(I) discrete complexes and coordination polymers with pyridyl ligands have been reported,[6,7] owing to the excellent affinity of Ag(I) ions for N-donor ligands and their highly flexible coordination geometry, which can vary from linear[8] to trigonal,[9] tetrahedral,[10] square-planar,[11] trigonal pyramidal,[12] T-shaped,[13] and octahedral.[14] In addition, adjacent metal centers in multinuclear Ag(I) complexes may form argentophilic closed-shell interactions,[15] which significantly influence a supramolecular topology and photophysical characteristics of the complexes, such as luminescence.[16] A conformationally flexible ligand based on the 2,2′-bipyridine motif was used to prepare a series of 1D and 2D Ag(I) coordination polymers having different topologies, which were dictated by the choice of different counteranions and solvents.[17] 2,2′-Bipyridine was also found to be the ligand of choice to ensure an appropriate environment for the stabilization of Ag(II) ions, as reported by Kandaiah et al.[18] Multimetallic Ag(I)-pyridyl complexes have found potential applications as photoactive materials,[19] biologically active agents,[20] and catalysts.[21] For instance, a dinuclear Ag(I) complex containing tris(2-pyridyl)phosphine ligands shows blue thermally activated fluorescence,[22] while a disilver(I) compound with a terpyridine ligand efficiently catalyzes the aziridination of olefins.[23] Two dipyridylquinoxaline-type ligands coordinated to two Ag(I) ions by using three nitrogen atoms of each ligand to form discrete boxlike dimers with promising redox and luminescent properties.[24] Interestingly enough, the reaction of hexakis(2-pyridyl)[3]radialene with $AgBF_4$ resulted in the formation of a hexapodal metallosupramolecular assembly of the M_6L_2 type with an encapsulated fluoride anion.[25]

Molecules based on the hexaarylbenzene[26] core containing multiple donor sites appear to be attractive in the development of new coordination building blocks due to their unique propeller-shaped topology. Recently, we have reported a microwave-promoted synthesis of hexaheteroarylbenzenes based on a multiple iterative C−H activation protocol and preliminary results of their complexation with Ru(II), Pd(II), and Pt(II) atoms to give only dinuclear complexes.[27] Thus, a new easy access to hexaarylbenzene ligands offers options for novel metal-driven self-assembled architectures, such as thiazole-containing hexaarylbenzenes, which were utilized in

Received: December 18, 2019
Published: March 5, 2020

https://dx.doi.org/10.1021/acs.inorgchem.9b03664
Inorg. Chem. 2020, 59, 3993−4001

Scheme 1[a]

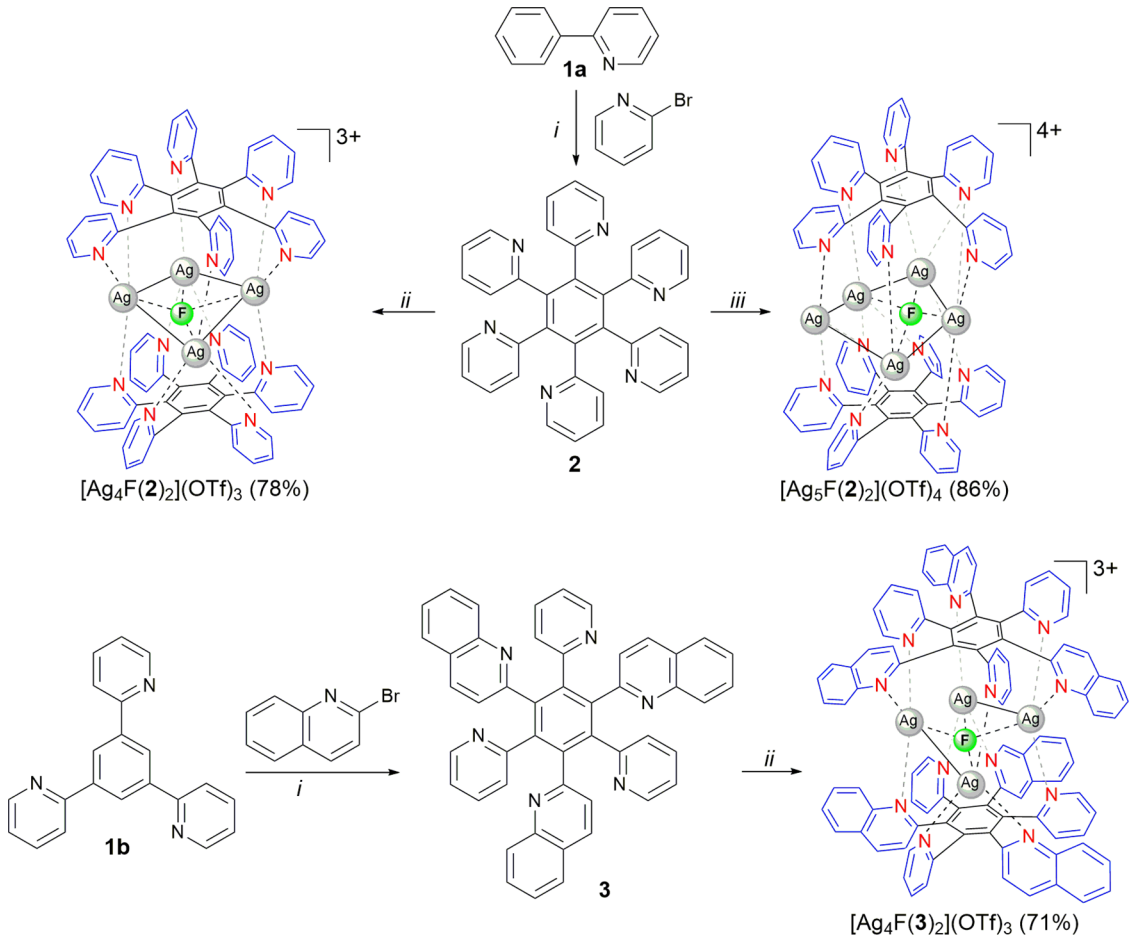

[a]Reaction conditions: (i),[27] (ii) **2** or **3** (0.05 mmol), AgOTf (0.075 mmol), AgF (0.025 mmol), MeOH (1 mL), rt in the dark 12 h; (iii) **2** (0.05 mmol), AgOTf (0.125 mmol), AgF (0.025 mmol), MeOH (1 mL), rt in the dark 12 h.

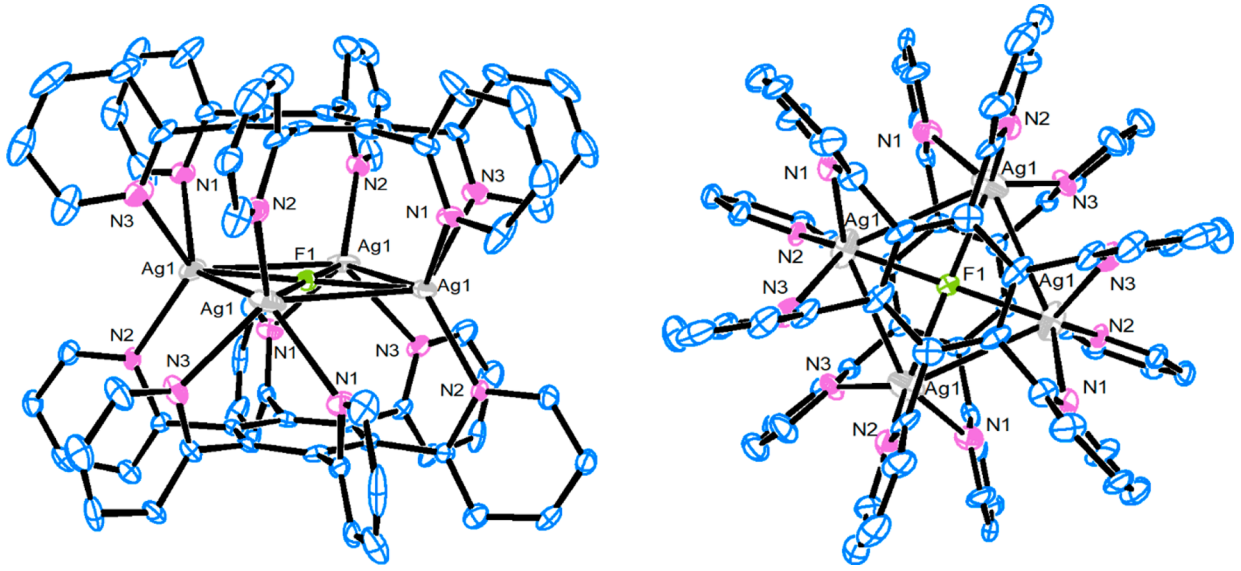

Figure 1. X-ray structure of the $[Ag_4F(\mathbf{2})_2]^{3+}$ cation. Hydrogen atoms have been omitted for clarity.

complexation with Ag(I) and Pt(II) ions to assemble molecular rotors.[28] The Shionoya group designed a tris-monodentate hexaarylbenzene-type ligand with three alternately attached 3-pyridyl and *p*-tolyl groups, which was used in the preparation of capsule-shaped and cage-shaped complexes via self-assembly of four ligand molecules and four or six Ag(I) ions.[29] Lee and co-workers reported monomeric dinuclear Cu(I) and Cu(II) complexes with hexakis(2-pyridyl)benzene

https://dx.doi.org/10.1021/acs.inorgchem.9b03664
Inorg. Chem. 2020, 59, 3993−4001

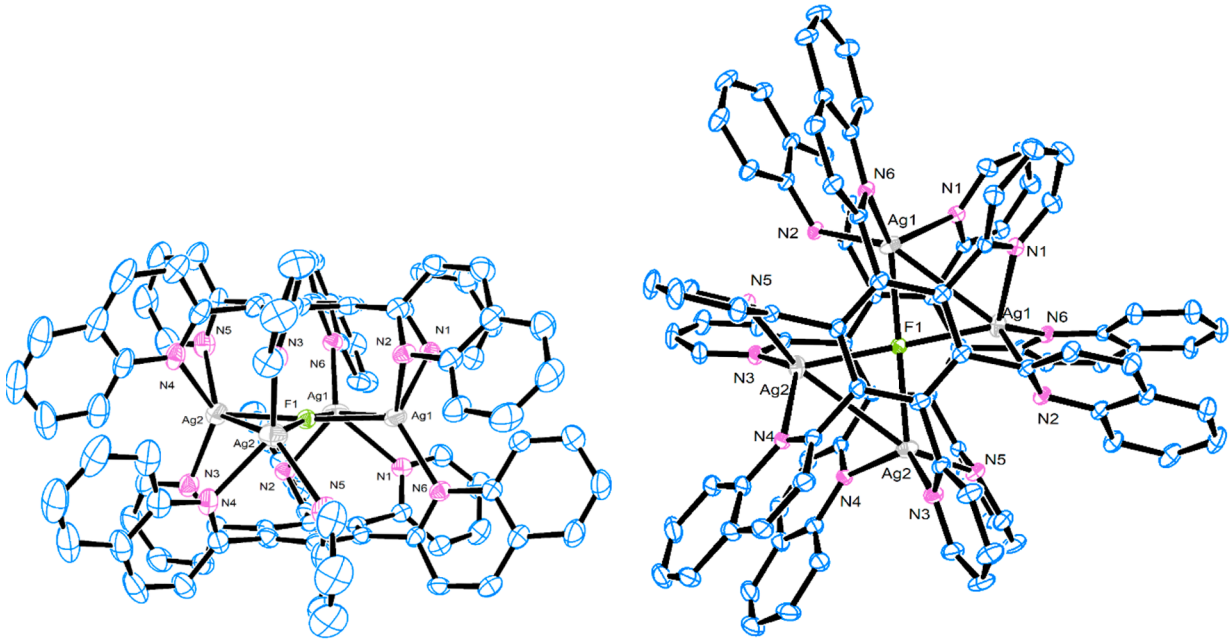

Figure 2. X-ray structure of $[Ag_4F(\mathbf{3})_2]^{3+}$. Hydrogen atoms have been omitted for clarity.

derivatives, which exhibited the fluxional motion of two copper ions.[30] However, the chemistry of Ag(I) coordination complexes based on hexakis(heteroaryl)benzene ligands with six N-donor sites is still unexplored.

Taking into account our previous work on the complexation of a hexakis(pyridin-2-yl)benzene ligand (**2**) with selected transition metals,[27] we envisioned that hexakis(azaheteroaryl)-benzene-type ligands could interact with Ag(I) ions so as to minimize electrostatic repulsion between positively charged metal centers. Herein we describe, on the basis of a unique cooperation of ligands hexakis(pyridin-2-yl)benzene (**2**) and 2,4,6-tris(pyridin-2-yl)-1,3,5-tris(quinolin-2-yl)benzene (**3**) with fluoride anion inclusion and argentophilic interactions, the synthesis and complete characterization of three novel unexpected multinuclear Ag(I)-polypyridyl cationic complexes: $[Ag_4F(\mathbf{2})_2]^{3+}$, $[Ag_4F(\mathbf{3})_2]^{3+}$, and $[Ag_5F(\mathbf{2})_2]^{4+}$.

RESULTS AND DISCUSSION

Hexakis(azaheteroaryl)benzene ligands **2** and **3** were readily synthesized from coupling reactions of 2-phenylpyridine (**1a**) and 1,3,5-tris(pyridin-2-yl)benzene (**1b**) with 2-bromopyridine or 2-bromoquinoline via Ru(II)-catalyzed multiple C−H functionalization under microwave conditions in water (Scheme 1).[27]

To investigate the coordination properties of the synthesized propeller-like ligands with Ag(I) ions, the ligand **2** was first treated with 3 equiv of AgOTf in MeOH at room temperature in the dark for 12 h. A white solid, isolated by MeOH/Et_2O precipitation, was a mixture of products according to ^{1}H NMR analysis in a deuterated acetone solution. However, after slow evaporation of acetone a few crystals were formed and were suitable for X-ray analysis. We were able to elucidate the stoichiometry of the complex from diffraction data, which was additionally confirmed by elemental analysis. To our surprise, the crystallized compound contained four Ag(I) ions in the sandwich-type cationic $[Ag_4F(\mathbf{2})_2]^{3+}$ complex with two pyridyl ligands **2** arranged facetoface, and a fluoride anion coordinated in the middle of the square formed by Ag(I) ions (Figure 1). The six pyridyl nitrogen atoms of both ligands **2** in $[Ag_4F(\mathbf{2})_2](OTf)_3$ interact with the highly positively charged $[Ag_4F]^{3+}$ nucleus of the complex. Similarly, Lu et al. reported Ag_4L_2 metallocage structures with trapped nitrate anions as a result of self-assembly of $AgNO_3$ with tetratopic 1,2,4,5-tetrakis(benzoimidazolylmethyl)benzene ligands.[31]

At this stage, the source of the fluoride anions remains unknown, but we speculate that they were present as an impurity in AgOTf and thus actively participated in the thermodynamically favorable self-assembly process. This hypothesis could actually explain the initially observed formation of the crystalline complex $[Ag_4F(\mathbf{2})_2](OTf)_3$ in a small amount. After the complex stoichiometry was revealed ($[Ag^+]/[\mathbf{2}]/[F^-]$ ratio 4/2/1), the ligand **2** was mixed with 1.5 equiv of AgOTf and 0.5 equiv of AgF, giving the pure complex $[Ag_4F(\mathbf{2})_2](OTf)_3$ in 78% isolated yield. The solution structure of the complex was revealed by ^{1}H NMR spectroscopy and ESI-HRMS measurements (m/z 509.0100, 837.9912, 1824.9325: $[Ag_4F(\mathbf{2})_2]^{3+}$, $[Ag_4F(\mathbf{2})_2OTf]^{2+}$, and $[Ag_4F(\mathbf{2})_2(OTf)_2]^+$, respectively).

The ^{1}H NMR spectrum of $[Ag_4F(\mathbf{2})_2](OTf)_3$ in acetone-d_6 shows only one set of four signals corresponding to pyridyl groups of both coordinated ligands **2** in the same environment. The pyridyl H-3, H-4, and H-5 proton signals are expectedly shifted downfield in comparison to the free ligand **2**, as a result of a loss in electron density upon coordination to Ag(I) ions (Figure 3a,b). In contrast, the resonance of the H-6 proton, which is in closest proximity to the metal binding site, remained unchanged. It can be seen from the solid-state structure of the complex that the two ligands **2** arranged face to face are rotated with respect to each other so that the pyridine ring of one ligand molecule is oriented toward the region between two pyridine rings of another ligand molecule (Figure 1). Thus, all pyridine rings are approximately parallel and the H-6 protons are pointing close to the shielding cones caused by the motion of the π electrons in pyridine rings (Figure S45).

https://dx.doi.org/10.1021/acs.inorgchem.9b03664
Inorg. Chem. 2020, 59, 3993−4001

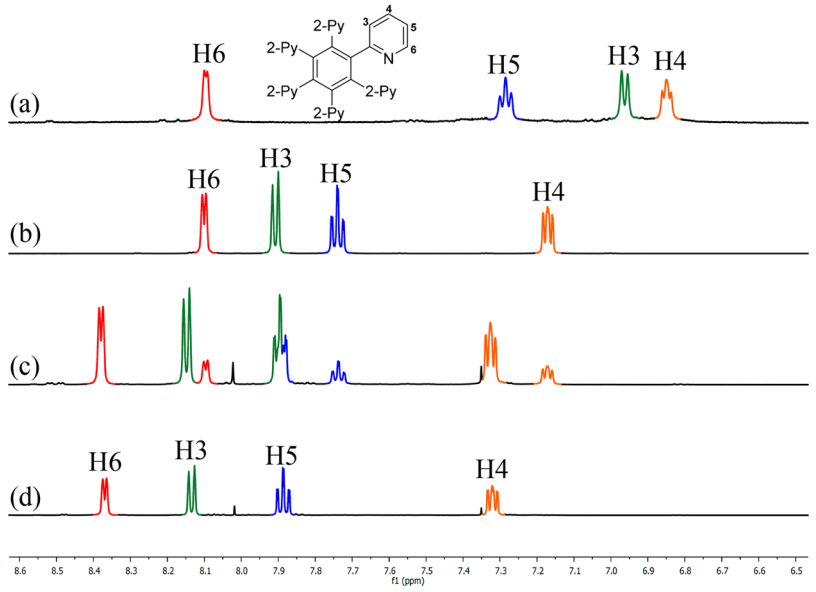

Figure 3. ^{1}H NMR spectra (500 MHz, acetone-d_6, 296 K): (a) free ligand **2**; (b) pure $[Ag_4F(\mathbf{2})_2](OTf)_3$; (c) mixture of $[Ag_5F(\mathbf{2})_2](OTf)_4$ and $[Ag_4F(\mathbf{2})_2](OTf)_3$ resulting from 2/1/1 [AgOTf]/[**2**]/[AgF]; (d) pure $[Ag_5F(\mathbf{2})_2](OTf)_4$.

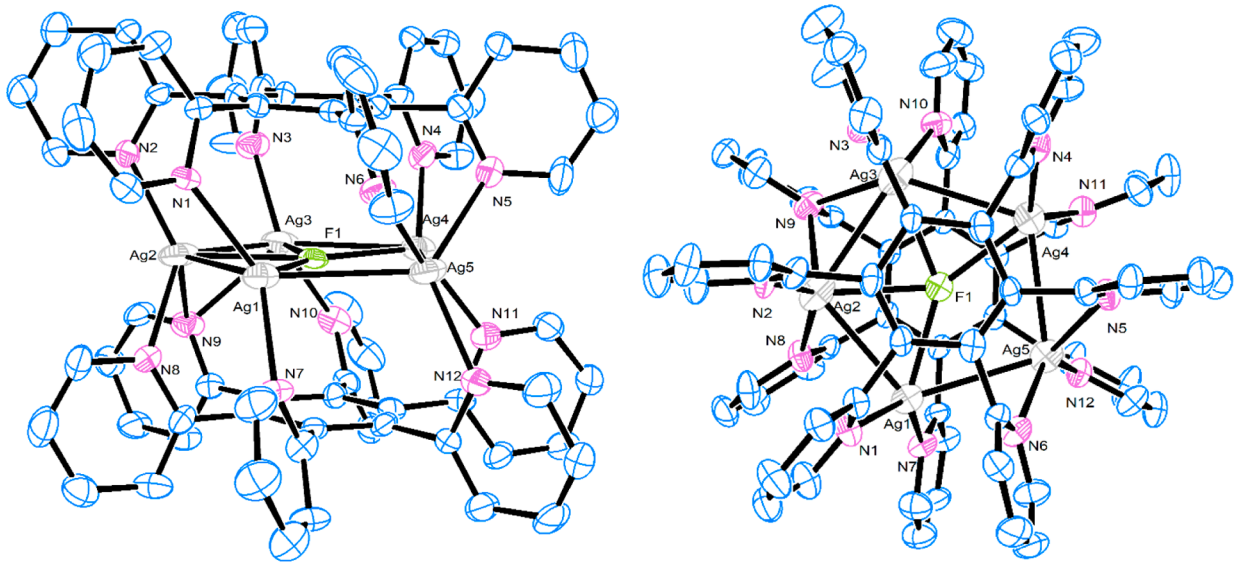

Figure 4. X-ray structure of $[Ag_5F(\mathbf{2})_2]^{4+}$. Hydrogen atoms have been omitted for clarity.

Presumably, the H-6 proton resonance experiences a downfield shift due to the electron-withdrawing effect of the Ag(I) ion which cancels out with the upfield shift attributed to an anisotropy effect of the pyridyl groups,[32] and consequently it remains unchanged.

The importance of fluoride anions for the successful generation of the supramolecular structure was additionally illustrated by reactions of ligand **2** with 2 equiv of $AgPF_6$ or $AgSbF_6$, which led to mixtures of products. On the other hand, the combination of $AgPF_6$ or $AgSbF_6$ with AgF in a 3:1 molar ratio again yielded the pure complexes $[Ag_4F(\mathbf{2})_2](PF_6)_3$ and $[Ag_4F(\mathbf{2})_2](SbF_6)_3$, as confirmed by comparison of their ^{1}H NMR spectra with that resulting from the $[Ag_4F(\mathbf{2})_2](OTf)_3$ complex. It is worth mentioning that the reaction of ligand **2** with 2 equiv of AgF solely furnished a mixture of products, indicating that the presence of weakly coordinating counterions, such as TfO^-, SbF_6^-, and PF_6^-, is not negligible in the self-assembly process.

The isostructural tetranuclear complex $[Ag_4F(\mathbf{3})_2](OTf)_3$ but with the hybrid quinolinyl-pyridyl ligand **3** was prepared and isolated in 71% yield by reacting **3** (1 equiv), AgOTf (1.5 equiv), and AgF (0.5 equiv). Its solid-state structure was unambiguously determined by X-ray analysis revealing a symmetric sandwich-type complex analogous to $[Ag_4F(\mathbf{2})_2](OTf)_3$ (Figure 2).

An MS-ESI analysis provided the nature of ions characteristic of the complex $[Ag_4F(\mathbf{3})_2](OTf)_3$ present in solution, which were verified by comparison of the isotopic patterns between observed and simulated peaks (Supporting Information). The major peaks correspond to $[Ag_4F(\mathbf{3})_2]^{3+}$, $[Ag_4F(\mathbf{3})_2OTf]^{2+}$, and $[Ag_4F(\mathbf{3})_2(OTf)_2]^+$ species, indicating the presence of a multinuclear structure also in solution. While the solid-state structure of $[Ag_4F(\mathbf{3})_2](OTf)_3$ indicates two slightly different pyridine and quinoline environments (Figure 2), a highly symmetric structure in acetone-d_6 solution was evidenced by ^{1}H NMR spectroscopy, which displayed only

https://dx.doi.org/10.1021/acs.inorgchem.9b03664
Inorg. Chem. 2020, 59, 3993−4001

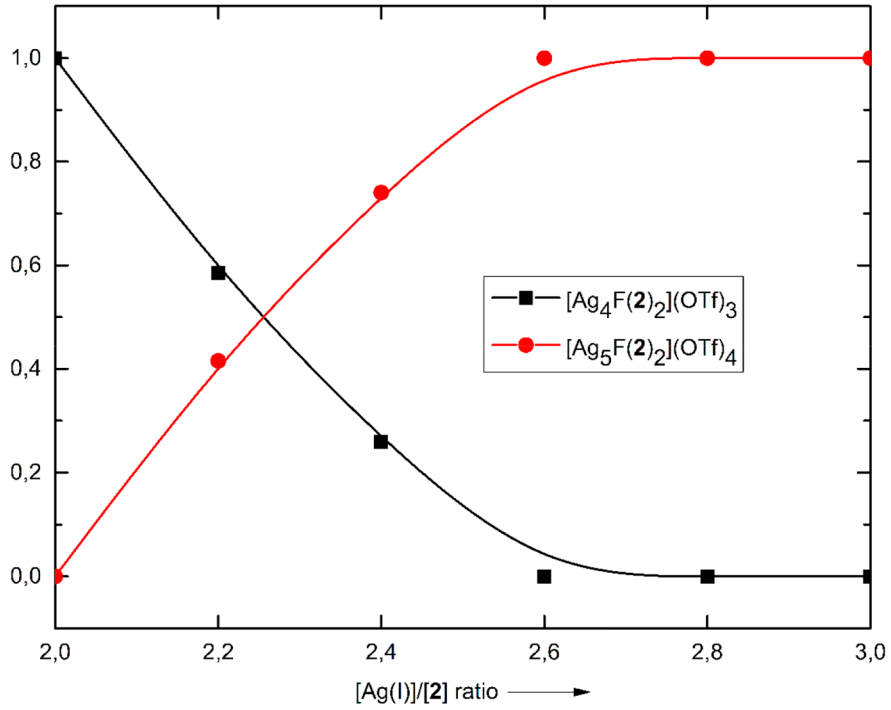

Figure 5. Proportions of Ag(I) complexes in crude reaction mixtures as a function of different [Ag(I)]/[**2**] ratios, determined by ^{1}H NMR spectroscopy.

one set of resonances for pyridyl and quinolinyl groups in both coordinated ligands **3**. Variable-temperature ^{1}H NMR measurements (240 → 300 K) of the complex $[Ag_4F(\mathbf{3})_2](OTf)_3$ in acetone-d_6 showed no signal doubling or line broadening (Figure S4). These observations suggest a dynamic process in solution, which, however, cannot be suppressed by cooling to only 240 K.

We speculated that more than four Ag(I) ions could coordinate to the ligand **2** by simply changing the [**2**]/[Ag^+]/[F^-] ratio. Indeed, when the ligand **2** was treated with 2 equiv of AgOTf and 1 equiv of AgF, in addition to the proton signals for ligand **2** incorporated in the complex $[Ag_4F(\mathbf{2})_2](OTf)_3$, another set of signals appeared in a symmetrical pattern (Figure 3c). All four new pyridyl signals are shifted downfield by 0.15−0.27 ppm relative to resonances of the ligand **2** in the complex $[Ag_4F(\mathbf{2})_2](OTf)_3$. This indicated a decrease in electron density upon coordination of the nitrogen lone pair to the silver metal center and suggested a highly positively charged species. After the amounts of silver salts were changed to 2.5 equiv of AgOTf and 0.5 equiv of AgF, the pure complex $[Ag_5F(\mathbf{2})_2](OTf)_4$ was isolated by MeOH/Et_2O precipitation in 86% yield.

The structure of the complex $[Ag_5F(\mathbf{2})_2](OTf)_4$ was determined by X-ray crystallography and revealed that the pentagonal unit of Ag(I) ions with a centrally included fluoride anion is coordinated to both ligands **2** in a symmetrical sandwich-shaped structure (Figure 4). This is consistent with the four proton signals of the coordinated ligand **2** indicating a highly symmetrical structure also in solution (Figure 3d). It is worth noting that, while four Ag(I) ions are retained in the pentanuclear complex via coordination to both polydentate ligand molecules and a fluoride anion, the fifth Ag(I) ion has interactions with only pyridyl nitrogens.

To investigate the formation of different complexes, reactions of ligand **2**, 0.5 equiv of AgF, and 1.5−2.5 equiv of AgOTf were performed, and crude reaction mixtures were analyzed by ^{1}H NMR spectroscopy (Figure 5). When the total amount of Ag(I) ions (from AgF and AgOTf) surpassed 2 equiv relative to the ligand **2**, the molar portion of the complex $[Ag_4F(\mathbf{2})_2](OTf)_3$ in the reaction mixture started to decrease, and simultaneously the amount of the product with five coordinated Ag(I) ions started to increase. Once the molar ratio [Ag(I)]/[**2**] reached 2.6 (2.1 equiv of AgOTf and 0.5 equiv of AgF), the complex $[Ag_5F(\mathbf{2})_2](OTf)_4$ was formed as the sole product regardless of the additional amount of AgOTf.

The aforementioned results indicate that the self-assembly process can be regulated by a subtle choice of [Ag(I)]/[**2**] ratio and more importantly imply a possible structure interconversion (Figure 6). Indeed, the complex $[Ag_5F(\mathbf{2})_2](OTf)_4$ can be easily formed from a methanolic solution of $[Ag_4F(\mathbf{2})_2](OTf)_3$ by adding a 1.5-fold excess of AgOTf, and it was isolated by MeOH/Et_2O precipitation in 61% yield. On the other hand, if the pentanuclear complex $[Ag_5F(\mathbf{2})_2](OTf)_4$ was treated with water for 0.5 h at room temperature, the tetranuclear complex $[Ag_4F(\mathbf{2})_2](OTf)_3$ was isolated in 72% yield. As evidenced by the X-ray structure of $[Ag_5F(\mathbf{2})_2](OTf)_4$, one Ag(I) ion is not coordinated to the fluoride anion, and thus it can more easily dissociate from the complex due to the relatively weak Ag−N bond.[33] The MS-ESI spectrum of

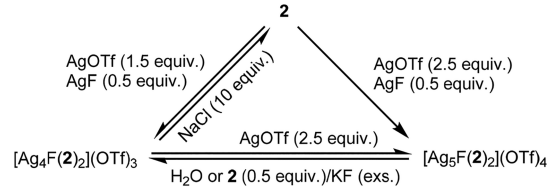

Figure 6. Interconversions among tetra- and pentanuclear complexes and ligand **2**.

https://dx.doi.org/10.1021/acs.inorgchem.9b03664
Inorg. Chem. 2020, 59, 3993−4001

$[Ag_5F(\mathbf{2})_2](OTf)_4$ showed only peaks for the main ions originating from the complex $[Ag_4F(\mathbf{2})_2](OTf)_4$ ($[Ag_4F(\mathbf{2})_2]^{3+}$, $[Ag_4F(\mathbf{2})_2TfO]^{2+}$, and $[Ag_4F(\mathbf{2})_2(TfO)_2]^{+}$), additionally supporting the lability of one Ag(I) ion in solution (Supporting Information). Addition of ligand **2** (0.5 equiv) and a large excess of KF to the methanolic solution of $[Ag_5F(\mathbf{2})_2](OTf)_4$ induced its rearrangement into the complex $[Ag_4F(\mathbf{2})_2](OTf)_3$, which was isolated in 80% yield. Notably, both complexes are stable in an N-coordinating solvent, such as acetonitrile, but the complex $[Ag_4F(\mathbf{2})_2](OTf)_3$ quantitatively released the polydentate ligand **2** in the presence of chloride anions in methanol. This implies that chloride anions are not able to replace a fluoride anion via dissociation/association steps but rather they abstract Ag(I) ions by forming a less soluble AgCl salt.

Structural Analyses of Complexes. *Structural Analysis of $[Ag_4F(\mathbf{2})_2](OTf)_3$.* The crystallographic analysis revealed that the complex crystallizes in the *Pnnn* space group. The complex has a 3D sandwichlike shape with four silver ions forming a square between two ligands **2**. In both ligands, all six pyridine rings are directed toward the center of the complex with torsion angles from 83.5(4) to 85.4(4)°. Silver ions are coordinated with three pyridine nitrogen atoms and one fluoride anion. If the Ag···Ag interaction is neglected, the geometry around silver is almost tetrahedral. The distortion from perfect tetrahedral geometry can be determined by using the $\tau 4$ geometry index: $\tau 4 = (360 - (\alpha + \beta))/141$. The α and β values presented in the equation are the largest angles around the metal center. Values for $\tau 4$ vary from 1 for a perfectly tetrahedral to 0 for a perfectly square planar geometry.[34] The $\tau 4$ value for Ag1 is 0.86, which can be considered as an almost perfect tetrahedral coordination geometry. The distances for the Ag−N bonds are in the range from 2.216(6) to 2.427(8) Å, and the Ag−F distance is 2.3204(8) Å. A crystal structure also revealed the Ag···Ag interactions. The distances between two silver ions are 3.195(2) and 3.366(2) Å, which are shorter than the sum of two silver van der Waals radii (3.44 Å), indicating the presence of two strong and two weak argentophilic interactions in the complex cation.[15,35] Moreover, in the middle of the complex is F^-, which is coordinated to four silver atoms (2.3204(8) Å). The anion is 3.081 Å from the benzene rings, thus indicating an anion−π interaction which is normally in the range 2−5 Å.[36,37] Nevertheless, the F^- anion enables the tetrahedral coordination around the silver atom and also partially neutralizes the positive charge which is a consequence of four silver cations in the close-packed complex.

Structural Analysis of $[Ag_4F(\mathbf{3})_2](OTf)_3$. The complex crystallizes in the trigonal $P3_221$ space group. The complex has the same sandwichlike shape and four silver ions in an almost square orientation coordinated by two ligands **3** as in $[Ag_4F(\mathbf{2})_2](OTf)_3$. The pyridine and quinoline rings deviate from the benzene ring from 61.1(3) to 86.5(4)° and from 62.7(3) to 71.5(3)°, respectively. Ag1 is coordinated by one pyridine and two quinoline nitrogen atoms and a fluoride anion, while Ag2 is coordinated by two pyridine and one quinoline nitrogen atom and a fluoride anion. The distortions from a perfectly tetrahedral geometry determined by $\tau 4$ are 0.83 and 0.84 for Ag1 and Ag2, respectively, indicating almost perfect tetrahedral coordination geometry (if the Ag···Ag interactions are neglected). The distances for the Ag−N_{Py} bonds are in the range from 2.249(5) to 2.491(5) Å and for the Ag−N_{Quin} bonds from 2.242(4) to 2.525(5) Å. The distances for Ag1···Ag1 and Ag2···Ag2 are 3.1171(9) and 3.2036(9) Å, respectively, and are shorter than the sum of van der Waals radii (3.44 Å). This indicates strong argentophilic interactions, while the Ag1···Ag2 distance is 3.5703(6) Å and is longer than sum of van der Waals radii, which means that there is no argentophilic interaction. The F^- anion in the center of the complex is coordinated to four silver atoms with Ag1−F and Ag2−F distances of 2.351(3) and 2.413(3) Å, respectively. On the other hand, F^- is 2.961 Å from the benzene rings, thus indicating an anion−π interaction.

Structural Analysis of $[Ag_5F(\mathbf{2})_2](OTf)_4$. The complex crystallizes in the monoclinic $P2_1/n$ space group. The complex has the same sandwichlike shape as $[Ag_4F(\mathbf{2})_2](OTf)_3$ and $[Ag_4F(\mathbf{3})_2](OTf)_3$ but with five silver ions in an almost pentagonal orientation coordinated by two ligands **2**. The pyridine rings deviate from the benzene ring from 68.1(2) to 89.6(6)°. The Ag2, Ag3, and Ag4 silver ions are coordinated by three pyridine nitrogen atoms and a fluoride anion ($\tau 4 = 0.80$) and Ag1 is coordinated by two pyridine nitrogen atoms and an F^- anion while Ag5 is coordinated only by three pyridine nitrogen atoms (Ag5···F1 = 2.724(9) Å). Distances for Ag−N bonds are in the range from 2.201(9) to 2.714(11) Å. The distances for Ag···Ag are 2.9388(14)−3.0845(16) Å and are shorter than sum of van der Waals radii (3.44 Å), indicating strong argentophilic interactions. The F^- in the center of the complex is coordinated on four silver atoms with Ag−F distances of 2.397(7)−2.575(7) Å. The distances between F^- and benzene rings (2.971 and 2.980 Å) indicate anion−π interactions.

CONCLUSIONS

In summary, we have demonstrated that hexakis(heteroaryl)benzenes **2** and **3**, bearing six radially extended nitrogen-coordinating groups, can serve as polydentate ligands (L) for the construction of multinuclear silver(I) sandwich-shaped complexes of the types Ag_4FL_2 and Ag_5FL_2. Generation of the complexes $[Ag_4F(\mathbf{2})_2](OTf)_3$, $[Ag_4F(\mathbf{3})_2](OTf)_3$, and $[Ag_5F(\mathbf{2})_2](OTf)_4$ is initiated by a unique cooperation of ligand molecules, argentophilic interactions, and fluoride anion coordination in a self-assembled manner. The tetranuclear and pentanuclear complexes consist of Ag_4 and Ag_5 planar units with a centrally coordinated fluoride anion, located between two polydentate ligand molecules pointing all six of their nitrogen atoms toward the Ag_4F or Ag_5F plane. The reactions of ligands with AgX (X = OTf, PF_6, SbF_6) or AgF solely led to mixtures of products, indicating that the selective formation of the complexes is dictated by an appropriate choice of $[L]/[Ag^+]/[F^-]$ ratio and noncoordinating counteranion. To the best of our knowledge, we have presented here the first examples of coordination complexes containing a highly positively charged $[Ag_4F]^{3+}$ or $[Ag_5F]^{4+}$ nucleus between two hexa(azaheteroaryl)benzene ligands. Interconversion between tetrasilver(I) and pentasilver(I) compounds was also demonstrated. The selectively prepared cationic species $[Ag_4F(\mathbf{2})_2]^{3+}$, $[Ag_4F(\mathbf{3})_2]^{3+}$, and $[Ag_5F(\mathbf{2})_2]^{4+}$ offer a potential for catalytic applications that are currently being evaluated.

EXPERIMENTAL SECTION

General Methods. All reagents were commercial grade and were used without further purification. The ligands **2** and **3** were prepared as previously reported by our group.[27] NMR spectra were recorded with a Bruker Avance III 500 MHz spectrometer. The ^1H and ^{13}C NMR chemical shifts are reported in parts per million (ppm) relative to the central line of the acetone-d_6 signal (2.05 ppm for ^1H and 29.8

https://dx.doi.org/10.1021/acs.inorgchem.9b03664
Inorg. Chem. 2020, 59, 3993−4001

ppm for ^{13}C). The ^{19}F NMR chemical shifts are reported relative to the signal of trifluoromethylbenzene (−63.22 ppm). IR spectra were obtained with a Bruker ALPHA FT-IR spectrophotometer. High-resolution mass spectra were recorded with a Thermo Fisher Q-Exactive instrument, while mass spectra were recorded with a Micromass Waters Q-TOF Premier instrument. Elemental analyses (C, H, N) were performed with a PerkinElmer 2400 Series II CHNS/O Analyzer.

$[Ag_4F(2)_2](OTf)_3$. A screw-cap scintillation vial was loaded with ligand **2** (28 mg, 0.05 mmol), AgOTf (19.5 mg, 0.075 mmol), and AgF (3.4 mg, 0.025 mmol). The mixture was dissolved in 1 mL of MeOH and stirred in the dark at room temperature for 12 h. After that time Et_2O (2 mL) was added to precipitate the product, which was filtered off, washed with H_2O (1 mL) and Et_2O (2 × 1 mL), and dried to obtain the pure complex $[Ag_4F(2)_2](OTf)_3$ (38 mg, 0.0195 mmol, 78% yield) as a white solid. Mp: >300 °C dec. ^1H NMR (500 MHz, acetone-d_6): δ 8.10 (d, J = 5.0 Hz, 1H), 7.91 (d, J = 7.9 Hz, 1H), 7.74 (td, J = 7.7, 1.7 Hz, 1H), 7.17 (ddd, J = 7.6, 5.1, 1.3 Hz, 1H). ^{13}C NMR (126 MHz, acetone-d_6): δ 157.8, 150.3, 141.4, 138.7, 128.5, 124.1 121.6 (q, J = 322.0 Hz). ^{19}F NMR (471 MHz, acetone-d_6): δ −78.6 (OTf), −315.9 (F^-). IR (ATR): 1592, 1566, 1483, 1405, 1256, 1221, 1151, 1027, 997, 806, 754, 635 cm^{-1}. HR-MS (ESI): m/z calcd for $C_{72}H_{48}N_{12}FAg_4$ $[M - 3OTf]^{3+}$ 509.0099, found 509.0100. Anal. Calcd for $C_{75}H_{48}Ag_4F_{10}N_{12}O_9S_3 \cdot 3H_2O$: C, 44.31; H, 2.68; N, 8.27. Found: C, 44.25; H, 2.45; N, 8.19.

$[Ag_4F(3)_2](OTf)_3$. A screw-cap scintillation vial was loaded with ligand **3** (34.5 mg, 0.05 mmol), AgOTf (19.5 mg, 0.075 mmol), and AgF (3.4 mg, 0.025 mmol). The mixture was dissolved in 1 mL of MeOH and stirred in the dark at room temperature for 12 h. After that time Et_2O (2 mL) was added to precipitate the product, which was filtered off, washed with H_2O (1 mL) and Et_2O (2 × 1 mL), and dried to obtain the pure complex $[Ag_4F(3)_2](OTf)_3$ (40 mg, 0.018 mmol, 71% yield) as a white solid. Mp: >300 °C dec. ^1H NMR (500 MHz, acetone-d_6): δ 8.38 (d, J = 8.5 Hz, 1H), 8.27 (d, J = 8.5 Hz, 1H), 8.16 (dt, J = 7.9, 1.1 Hz, 1H), 8.03 (d, J = 5.0 Hz, 1H), 7.84 (d, J = 7.9 Hz, 1H), 7.26 (ddd, J = 8.0, 6.9, 1.2 Hz, 1H), 7.01 (ddd, J = 7.6, 5.1, 1.3 Hz, 1H), 6.71 (d, J = 8.7 Hz, 1H), 6.52 (ddd, J = 8.5, 6.9, 1.3 Hz, 1H). ^{13}C NMR (126 MHz, acetone-d_6): δ 159.9, 158.1, 150.5, 146.2, 142.3, 141.5, 139.1, 139.0, 130.5, 129.0, 128.9, 128.5, 128.3, 127.8, 125.5, 124.3 121.6 (q, J = 322.0 Hz). ^{19}F NMR (471 MHz, acetone-d_6): δ −78.6 (OTf), −312.3 (F^-). IR (ATR): 1604, 1569, 1327, 1259, 1165, 1122, 1078, 1029, 1020, 868, 729, 637 cm^{-1}. ESI-MS: m/z for $C_{96}H_{60}Ag_4FN_{12}$ $[M - 3OTf]^{3+}$ 610.4. Anal. Calcd for $C_{99}H_{60}Ag_4F_{10}N_{12}O_9S_3$: C, 52.17; H, 2.65; N, 7.37. Found: C, 46.00; H, 2.35; N, 6.16.

$[Ag_5F(2)_2](OTf)_4$. A screw-cap scintillation vial was loaded with ligand **2** (28 mg, 0.05 mmol), AgOTf (32.5 mg, 0.125 mmol), and AgF (3.4 mg, 0.025 mmol). The mixture was dissolved in 1 mL of MeOH and stirred in the dark at room temperature for 12 h. After that time Et_2O (2 mL) was added to precipitate the product, which was filtered off, washed with H_2O (1 mL) and Et_2O (2 × 1 mL) and dried to obtain the pure complex $[Ag_5F(2)_2](OTf)_4$ (40 mg, 0.0215 mmol, 86% yield) as a white solid. Mp: >300 °C dec. ^1H NMR (500 MHz, acetone-d_6): δ 8.38 (d, J = 5.1 Hz, 1H), 8.15 (dt, J = 7.9, 1.2 Hz, 1H), 7.89 (td, J = 7.8, 1.6 Hz, 1H), 7.32 (ddd, J = 7.7, 5.2, 1.3 Hz, 1H). ^{13}C NMR (126 MHz, acetone-d_6): δ 157.3, 152.1, 141.9, 140.2, 129.7, 125.2 121.3 (q, J = 321.2 Hz). ^{19}F NMR (471 MHz, acetone-d_6): δ −78.7 (OTf), −284.5 (F^-). IR (ATR): 1592, 1565, 1434, 1405, 1258, 1221, 1150, 1028, 997, 806, 754, 635 cm^{-1}. ESI-MS: m/z for $C_{72}H_{48}Ag_4FN_{12}$ $[M - Ag - 3OTf]^{3+}$ 510.3. Anal. Calcd for $C_{76}H_{48}Ag_5F_{13}N_{12}O_{12}S_4 \cdot C_6H_6$: C, 42.56; H, 2.35; N, 7.26. Found: C, 42.85; H, 2.40; N, 7.86.

$[Ag_4F(2)_2]$ $(PF_6)_3$. A screw-cap scintillation vial was loaded with ligand **2** (28 mg, 0.05 mmol), $AgPF_6$ (19 mg, 0.075 mmol), and AgF (3.4 mg, 0.025 mmol). The mixture was dissolved in 1 mL of MeOH and stirred in the dark at room temperature for 12 h. After that time Et_2O (2 mL) was added to precipitate the product, which was filtered off, washed with H_2O (1 mL) and Et_2O (2 × 1 mL), and dried to obtain the pure complex $[Ag_4F(2)_2](PF_6)_3$ (48 mg, 0.0205 mmol, 82% yield) as a white solid. Mp: >300 °C dec. ^1H NMR (500 MHz, acetone-d_6): δ 8.14 (d, J = 5.1 Hz, 1H), 7.78 (td, J = 7.6, 1.6 Hz, 1H), 7.74 (dt, J = 7.7, 1.3 Hz, 1H), 7.21 (ddd, J = 7.4, 5.0, 1.5 Hz, 1H). ^{13}C NMR (126 MHz, acetone-d_6): δ 156.5, 149.8, 140.8, 138.1, 127.3, 123.4. ^{19}F NMR (471 MHz, acetone-d_6): δ −72.5 (d, $^1J_{FP}$ = 708.2 Hz, PF_6^-), −316.0 (F^-). IR (ATR): 1593, 1486, 1404, 875, 836, 807, 754 cm^{-1}. Anal. Calcd for $C_{72}H_{48}Ag_4F_{19}N_{12}P_3 \cdot 2H_2O$: C, 43.18; H, 2.63; N, 8.39. Found: C, 42.89; H, 2.30; N, 8.29.

$[Ag_4F(2)_2](SbF_6)_3$. A screw-cap scintillation vial was loaded with ligand **2** (28 mg, 0.05 mmol), $AgSbF_6$ (26 mg, 0.075 mmol), and AgF (3.4 mg, 0.025 mmol). The mixture was dissolved in 1 mL of MeOH and stirred in the dark at room temperature for 12 h. After that time Et_2O (2 mL) was added to precipitate the product, which was filtered off, washed with H_2O (1 mL) and Et_2O (2 × 1 mL), and dried to obtain the pure complex $[Ag_4F(2)_2](SbF_6)_3$ (45 mg, 0.02 mmol, 80% yield) as a white solid. Mp: >300 °C dec. ^1H NMR (500 MHz, acetone-d_6): δ 8.14 (d, J = 5.0 Hz, 1H), 7.86−7.70 (m, 2H), 7.21 (ddd, J = 7.4, 5.1, 1.5 Hz, 1H). ^{13}C NMR (126 MHz, acetone-d_6): δ 157.3, 150.7, 141.8, 139.0, 128.2, 124.3. ^{19}F NMR (471 MHz, acetone-d_6): δ −123.2 (superposition of a sextet due to $^{121}SbF_6^-$ and an octet due to $^{123}SbF_6^-$, $^1J_{F^{121}Sb}$ = 1941, $^1J_{F^{123}Sb}$ = 1051 Hz), −316.4 (F^-). IR (ATR): 1592, 1565, 1484, 1405, 997, 807, 753, 654 cm^{-1}. Anal. Calcd for $C_{72}H_{48}Ag_4F_{19}N_{12}Sb_3$: C, 38.61; H, 2.16; N, 7.51. Found: C, 38.50; H, 2.08; N, 7.44.

X-ray Crystallographic Studies. Crystal data for complexes $[Ag_4F(2)_2](OTf)_3$, $[Ag_4F(3)_2](OTf)_3 \cdot 3H_2O$, and $[Ag_5F(2)_2](OTf)_4 \cdot 2H_2O \cdot C_3H_6O \cdot C_6H_6$ were collected at 150 K on an Agilent Technologies SuperNova Dual diffractometer using monochromated Mo Kα radiation (λ = 0.71073 Å). The data were processed using CrysAlis Pro.[38] Structures were solved with the ShelXT[39] structure solution program using intrinsic phasing and refined by a full-matrix least-squares procedure based on F^2 with ShelXL[40] implemented in the Olex^2 program suite.[41] All non-hydrogen atoms were readily located and refined anisotropically unless otherwise noted. Hydrogen atoms were initially located in the difference Fourier maps and were subsequently included in the model at geometrically calculated positions and refined by using a riding model unless otherwise noted. For $[Ag_4F(2)_2](OTf)_3$ the complex cation was readily located and refined; however, only a few atoms of the counterions were located, having very large anisotropic displacement parameters, and were in further steps of the refinement removed from the model. The scattering contributions of the disordered counterions were removed with a solvent mask procedure implemented in Olex^2. The counterion contribution was not included in the reported molecular weight and density. Although the crystals were of low quality (R_{int} = 0.1833), the data were of sufficient quality to determine the structure of the complex cation. In the structure of $[Ag_4F(3)_2](OTf)_3 \cdot 3H_2O$ hydrogen atoms on water oxygen atoms were not found in difference Fourier maps and were not included in the refinement. One water molecule and one triflate anion were disordered over a 2-fold rotation axis in the fixed ratio 0.50/0.50. Water molecules O8−O10 were refined with a fixed occupancy of 0.33 and restrained U_{ij} components. Hydrogen atoms attached to water molecules O1 and O8−O10 were not found in Fourier difference maps and were not included in the model. Crystals of$[Ag_5F(2)_2](OTf)_4 \cdot 2H_2O \cdot C_3H_6O \cdot C_6H_6$ were obtained by recrystallization from an acetone/benzene/ethyl acetate mixture, and the crystal structure contains electron density that belongs to disordered solvate molecules. One triflate anion was refined by fixing the coordinates of C76 and O11 and restraining U_{ij} components for O11, C76, F12, and F13. Benzene solvate molecule atoms C80−C85 were refined isotropically, and hydrogen atoms were not included in the model. Water molecules O14 and O16 were refined with a fixed occupancy ratio of 0.50 and restrained U_{ij} components. Hydrogen atoms attached to water molecules O14−O16 were not found in Fourier difference maps and were not included in the model. The scattering contributions of the disordered solvate molecules, including the unrecognized C_4O_2 fragment, were removed with a solvent mask procedure implemented in Olex^2. The unmodeled solvent contribution was not included in the reported molecular weight and density. Although the crystals were of low quality and the wR2 values is 0.4596, the data were of sufficient quality to determine

https://dx.doi.org/10.1021/acs.inorgchem.9b03664
Inorg. Chem. 2020, 59, 3993−4001

the molecular and crystal structure. Details of the crystal, data collection, and refinement parameters as well as selected bond distances and angles are given in Tables S1−S4 in the Supporting Information. The CCDC reference numbers are 1971156−1971158.

■ ASSOCIATED CONTENT

Supporting Information

The Supporting Information is available free of charge at https://pubs.acs.org/doi/10.1021/acs.inorgchem.9b03664.

Experimental procedures, tables of crystallographic details, NMR spectra, and MS spectra (PDF)

Accession Codes

CCDC 1971156−1971158 contain the supplementary crystallographic data for this paper. These data can be obtained free of charge via www.ccdc.cam.ac.uk/data_request/cif, or by emailing data_request@ccdc.cam.ac.uk, or by contacting The Cambridge Crystallographic Data Centre, 12 Union Road, Cambridge CB2 1EZ, UK; fax: +44 1223 336033.

■ AUTHOR INFORMATION

Corresponding Author

Franc Požgan − *Faculty of Chemistry and Chemical Technology, University of Ljubljana SI-1000 Ljubljana, Slovenia;* orcid.org/0000-0001-6040-294X; Email: franc.pozgan@fkkt.uni-lj.si

Authors

Miha Drev − *Faculty of Chemistry and Chemical Technology, University of Ljubljana SI-1000 Ljubljana, Slovenia;* orcid.org/0000-0002-8110-9248

Uroš Grošelj − *Faculty of Chemistry and Chemical Technology, University of Ljubljana SI-1000 Ljubljana, Slovenia*

Drago Kočar − *Faculty of Chemistry and Chemical Technology, University of Ljubljana SI-1000 Ljubljana, Slovenia*

Franc Perdih − *Faculty of Chemistry and Chemical Technology, University of Ljubljana SI-1000 Ljubljana, Slovenia;* orcid.org/0000-0002-8416-7291

Jurij Svete − *Faculty of Chemistry and Chemical Technology, University of Ljubljana SI-1000 Ljubljana, Slovenia;* orcid.org/0000-0003-3339-3595

Bogdan Štefane − *Faculty of Chemistry and Chemical Technology, University of Ljubljana SI-1000 Ljubljana, Slovenia*

Complete contact information is available at: https://pubs.acs.org/10.1021/acs.inorgchem.9b03664

Author Contributions

The manuscript was written through contributions of all authors. All authors have given approval to the final version of the manuscript.

Notes

The authors declare no competing financial interest.

■ ACKNOWLEDGMENTS

Financial support from the Slovenian Research Agency through grants P1-0179, P1-0175, and P1-0153 is gratefully acknowledged. We thank the EN-FIST Centre of Excellence, Dunajska 156, 1000 Ljubljana, Slovenia, for use of a Bruker Alpha FTIR spectrophotometer and Supernova diffractometer. Dr. D. Žigon (Jožef Stefan Institute, Ljubljana, Slovenia) is gratefully acknowledged for mass measurements. M.D. thanks the French government for a visitation grant for cooperative work at the University of Rennes (Centre régional de mesures physiques de l'Ouest).

■ DEDICATION

This paper is dedicated to Professor Marijan Kočevar, University of Ljubljana, on the occasion of his 70th birthday.

■ REFERENCES

(1) (a) Steel, P. J. Ligand Design in Multimetallic Architectures: Six Lessons Learned. *Acc. Chem. Res.* **2005**, *38* (4), 243−250. (b) Sinha, N.; Hahn, F. E. Metallosupramolecular Architectures Obtained from Poly-N-heterocyclic Carbene Ligands. *Acc. Chem. Res.* **2017**, *50* (9), 2167−2184. (c) Chakrabarty, R.; Mukherjee, P. S.; Stang, P. J. Supramolecular Coordination: Self-Assembly of Finite Two- and Three-Dimensional Ensembles. *Chem. Rev.* **2011**, *111* (11), 6810−6918. (d) Smulders, M. M. J.; Riddell, I. A.; Browne, C.; Nitschke, J. R. Building on architectural principles for three-dimensional metallosupramolecular construction. *Chem. Soc. Rev.* **2013**, *42* (4), 1728−1754.

(2) Glasson, C. R. K.; Lindoy, L. F.; Meehan, G. V. Recent developments in the d-block metallo-supramolecular chemistry of polypyridyls. *Coord. Chem. Rev.* **2008**, *252* (8−9), 940−963.

(3) (a) Xu, P.; Wang, G.; Zhu, Y.; Li, W.; Cheng, Y.; Li, S.; Zhu, C. Visible-Light Photoredox-Catalyzed C−H Difluoroalkylation of Hydrazones through an Aminyl Radical/Polar Mechanism. *Angew. Chem., Int. Ed.* **2016**, *55* (8), 2939−2943. (b) Zuo, Z.; MacMillan, D. W. C. DecarboxylativeArylation of α-Amino Acids via Photoredox Catalysis: A One-Step Conversion of Biomass to Drug Pharmacophore. *J. Am. Chem. Soc.* **2014**, *136* (14), 5257−5260. (c) Yasu, Y.; Koike, T.; Akita, M. Three-component oxytrifluoromethylation of alkenes: highly efficient and regioselectivedifunctionalization of C = C bonds mediated by photoredox catalysts. *Angew. Chem., Int. Ed.* **2012**, *51* (38), 9567−9571. (d) Xie, J.; Xu, P.; Li, H.; Xue, Q.; Jin, H.; Cheng, Y.; Zhu, C. A room temperature decarboxylation/C−H functionalization cascade by visible-light photoredox catalysis. *Chem. Commun.* **2013**, *49* (50), 5672−5674. (e) Gu, Z.; Zhang, H.; Xu, P.; Cheng, Y.; Zhu, C. Visible-Light-Induced Radical Tandem Aryldifluoroacetylation of Cinnamamides: Access to Difluoroacetylated Quinolone-2-ones And 1-Azaspiro[4.5]decanes. *Adv. Synth. Catal.* **2015**, *357* (14−15), 3057−3063.

(4) (a) Koike, T.; Akita, M. In *Ruthenium in Catalysis*; Bruneau, C., Dixneuf, P. H., Eds.; Springer: 2014; Topics in Organometallic Chemistry, pp 371−395. (b) Koike, T.; Akita, M. PhotoinducedOxyamination of Enamines and Aldehydes with TEMPO Catalyzed by $[Ru(bpy)_3]^{2+}$. *Chem. Lett.* **2009**, *38* (2), 166−167. (c) Nicewicz, D. A.; MacMillan, D. W. C. Merging Photoredox Catalysis with Organocatalysis: The Direct Asymmetric Alkylation of Aldehydes. *Science* **2008**, *322* (5898), 77−80. (d) Yasu, Y.; Koike, T.; Akita, M. Sunlight-driven synthesis of γ-diketones via oxidative coupling of enamines with silyl enol ethers catalyzed by $[Ru(bpy)_3]^{2+}$. *Chem. Commun.* **2012**, *48* (43), 5355−5357. (e) Yasu, Y.; Koike, T.; Akita, M. Intermolecular Aminotrifluoromethylation of Alkenes by Visible-Light-Driven Photoredox Catalysis. *Org. Lett.* **2013**, *15* (9), 2136−2139. (f) Renaud, P.; Leong, P. A Light Touch Catalyzes Asymmetric Carbon-Carbon Bond Formation. *Science* **2008**, *322* (5898), 55−56.

(5) Wang, C.-S.; Dixneuf, P. H.; Soulé, J.-F. Photoredox Catalysis for Building C−C Bonds from $C(sp^2)$−H Bonds. *Chem. Rev.* **2018**, *118* (16), 7532−7585.

(6) Njogu, E. M.; Omondi, B.; Nyamori, V. O. Review: Multimetallic silver(I)−pyridinyl complexes: coordination of silver(I) and luminescence. *J. Coord. Chem.* **2015**, *68* (19), 3389−3431.

(7) Khlobystov, A. N.; Blake, A. J.; Champness, N. R.; Lemenovskii, D. A.; Majouga, A. G.; Zyk, N. V.; Schröder, M. Supramolecular design of one-dimensional coordination polymers based on silver(I) complexes of aromatic nitrogen-donor ligands. *Coord. Chem. Rev.* **2001**, *222* (1), 155−192.

(8) Aguado, J. E.; Crespo, O.; Gimeno, M. C.; Jones, P. G.; Laguna, A.; Villacampa, M. D. Coordination properties of the 1,1′-bis[((6-

methyl)-2-pyridyl)amido]ferrocene ligand towards group 11 complexes. *DaltonTrans.* **2010**, *39* (18), 4321−4330.
(9) Al-Mandhary, M. R.; Fitchett, C. M.; Steel, P. J. Discrete Metal Complexes of Two Multiply Armed Ligands. *Aust. J. Chem.* **2006**, *59* (5), 307−314.
(10) Patra, G. K.; Goldberg, I. Coordination polymers of transition metal ions with polydentate imine ligands. Syntheses, materials characterization, and crystal structures of polymeric complexes of copper(I), silver(I) and zinc(II). *J. Chem. Soc., Dalton Trans.* **2002**, No. 6, 1051−1057.
(11) Hanton, L. R.; Young, A. G. Square-Planar Silver(I)-Containing Polymers Formed from π-Stacked Entities. *Cryst. Growth Des.* **2006**, *6* (4), 833−835.
(12) Yoon, I.; Lee, Y. H.; Jung, J. H.; Park, K.-M.; Kim, J.; Lee, S. S. Assembly of a tennis ball-like supramolecule coordinatively encapsulating disilver. *Inorg. Chem. Commun.* **2002**, *5* (10), 820−823.
(13) Broker, G. A.; Tiekink, E. R. Bis(μ-pyridine-1-carbaldehyde azine-$\kappa^2N,N':\kappa^2N'',N'''$)disilver(I) bis-(methane-sulfonate). *Acta Crystallogr., Sect. E: Struct. Rep. Online* **2007**, *63*, No. m2368.
(14) Han, L.; Chen, Z.; Luo, J.; Hong, M.; Cao, R. Hexa-kis-(μ_3-pyridine-2-thiol-ato-$\kappa^3N:S:S$)-hexasilver(I), $[Ag_6(\mu_3\text{-}SPy)_6]$. *Acta Crystallogr., Sect. E: Struct. Rep. Online* **2002**, *58*, m383−m384.
(15) Schmidbaur, H.; Schier, A. Argentophilic Interactions. *Angew. Chem., Int. Ed.* **2015**, *54* (3), 746.
(16) Liu, X.; Guo, G.-C.; Fu, M.-L.; Liu, X.-H.; Wang, M.-S.; Huang, J.-S. Three Novel Silver Complexes with Ligand-Unsupported Argentophilic Interactions and Their Luminescent Properties. *Inorg. Chem.* **2006**, *45* (9), 3679−3685.
(17) Gupta, A. K.; Salazar, D. M.; Orthaber, A. Solvent and Counter-Ion Induced Coordination Environment Changes TowardsAg^I Coordination Polymers. *Eur. J. Inorg. Chem.* **2019**, *2019* (33), 3740−3744.
(18) Kandaiah, S.; Huebner, R.; Jansen, M. Electrocrystallisation and single crystal structure determination of Bis(2,2′-bipyridyl)silver(II) perchlorate $[Ag(bipy)_2](ClO_4)_2$. *Polyhedron* **2012**, *48* (1), 68−71.
(19) Cheng, L.; Zhang, L.; Gou, S.; Cao, Q.; Wang, J.; Fang, L. Metal-directed one-dimensional chiral zigzag chains and right-handed 6_1 helix with multiple chiral components: luminescence and NLO properties. *CrystEngComm* **2012**, *14* (11), 3888−3893.
(20) (a) McDonnell, G.; Russell, A. D. Antiseptics and disinfectants: activity, action, and resistance. *Clin. Microbiol. Rev.* **1999**, *12* (1), 147−179. (b) Atiyeh, B. S.; Costagliola, M.; Hayek, S. N.; Dibo, S. A. Effect of silver on burn wound infection control and healing: review of the literature. *Burns* **2007**, *33* (2), 139−148. (c) Banti, C. N.; Hadjikakou, S. K. Anti-proliferative and anti-tumor activity of silver(I) compounds. *Metallomics* **2013**, *5* (6), 569−596.
(21) Li, Z.; He, C. Recent Advances in Silver-Catalyzed Nitrene, Carbene, and Silylene-Transfer Reactions. *Eur. J. Org. Chem.* **2006**, *2006* (19), 4313−4322.
(22) Artem'ev, A. V.; Shafikov, M. Z.; Schinabeck, A.; Antonova, O. V.; Berezin, A. S.; Bagryanskaya, I. Y.; Plusnin, P. E.; Yersin, H. Sky-blue thermally activated delayed fluorescence (TADF) based on Ag(I) complexes: strong solvation-induced emission enhancement. *Inorg. Chem. Front.* **2019**, *6* (11), 3168−3176.
(23) Cui, Y.; He, C. Efficient Aziridination of Olefins Catalyzed by a Unique Disilver(I) Compound. *J. Am. Chem. Soc.* **2003**, *125* (52), 16202−16203.
(24) Bu, X.-H; Liu, H.; Du, M.; Wong, K. M.-C.; Yam, V. W.-W.; Shionoya, M. Novel boxlike dinuclear or chain polymeric silver(I) complexes with polypyridyl bridging ligands: syntheses, crystal structures, and spectroscopic and electrochemical properties. *Inorg. Chem.* **2001**, *40* (17), 4143−4149.
(25) Steel, P. J.; Sumby, C. J. Hexa(2-pyridyl)[3]radialene: self-assembly of a hexanuclear silver array. *Chem. Commun.* **2002**, 322−323.
(26) Vij, V.; Bhalla, V.; Kumar, M. Hexaarylbenzene: Evolution of Properties and Applications of Multitalented Scaffold. *Chem. Rev.* **2016**, *116* (16), 9565−9627.
(27) Drev, M.; Grošlj, U.; Ledinek, B.; Perdih, F.; Svete, J.; Štefane, B.; Požgan, F. Ruthenium(II)-Catalyzed Microwave-Promoted Multiple C−H Activation in Synthesis of Hexa(heteroaryl)benzenes in Water. *Org. Lett.* **2018**, *20* (17), 5268−5273.
(28) (a) Hiraoka, S.; Hisanga, Y.; Shiro, M.; Shionoya, M. A molecular double ball bearing: an Ag(I)-Pt(II) dodecanuclear quadruple-decker complex with three rotors. *Angew. Chem., Int. Ed.* **2010**, *49* (9), 1669−1673. (b) Hiraoka, S.; Shiro, M.; Shionoya, M. Heterotopic Assemblage of Two Different Disk-Shaped Ligands through Trinuclear Silver(I) Complexation: Ligand Exchange-Driven Molecular Motion. *J. Am. Chem. Soc.* **2004**, *126* (4), 1214−1218. (c) Hiraoka, S.; Hirata, K.; Shionoya, M. A Molecular Ball Bearing Mediated by Multiligand Exchange in Concert. *Angew. Chem., Int. Ed.* **2004**, *43* (29), 3814−3818.
(29) Hiraoka, S.; Harano, K.; Shiro, M.; Shionoya, M. Quantitative dynamic interconversion between Ag(I)-mediated capsule and cage complexes accompanying guest encapsulation/release. *Angew. Chem., Int. Ed.* **2005**, *44* (18), 2727−2731.
(30) (a) Kwon, H.; Lee, E. Fluxional motion in a dinuclear copper(I) complex with a propeller-type ligand: metal hopping on both sides. *Dalton Trans.* **2018**, *47* (48), 17206−17210. (b) Kwon, H.; Lee, E. Static and dynamic coordination behaviours of copper(I) ions in hexa(2-pyridyl)benzene ligand systems. *Dalton Trans.* **2018**, *47* (25), 8448−8455. (c) Kwon, H.; Lee, E. Coordination preference of hexa(2-pyridyl)benzene with copper(ii) directed by hydrogen bonding. *CrystEngComm* **2018**, *20* (35), 5233−5240.
(31) Wu, J.-Y.; Lin, Y.-F.; Chuang, C.-H.; Tseng, T.-W.; Wen, Y.-S.; Lu, K.-L. Ag_4L_2Nanocage as a Building Unit toward the Construction of Silver Metal Strings. *Inorg. Chem.* **2008**, *47* (22), 10349−10356.
(32) Sahoo, H. S.; Chand, D. K.; Mahalakshmi, S.; Mir, M. H.; Raghunathan, R. Manifestation of diamagnetic chemical shifts of proton NMR signals by an anisotropic shielding effect of nitrate anions. *Tetrahedron Lett.* **2007**, *48* (5), 761−765.
(33) Wu, D.-Y.; Ren, B.; Jiang, Y.-X.; Xu, X.; Tian, Z.-Q. Density Functional Study and Normal-Mode Analysis of the Bindings and Vibrational Frequency Shifts of the Pyridine-M (M = Cu, Ag, Au, Cu^+, Ag^+, Au^+, and Pt) Complexes. *J. Phys. Chem. A* **2002**, *106* (39), 9042−9052.
(34) Addison, A. W.; Rao, T. N.; Reedijk, J.; van Rijn, J.; Verschoor, G. C. Synthesis, structure, and spectroscopic properties of copper(II) compounds containing nitrogen−sulphur donor ligands; the crystal and molecular structure of aqua[1,7-bis(*N*-methylbenzimidazol-2′-yl)-2,6-dithiaheptane]copper(II) perchlorate. *J. Chem. Soc., Dalton Trans.* **1984**, No. 7, 1349−1356.
(35) Pyykkö, P. Strong Closed-Shell Interactions in Inorganic Chemistry. *Chem. Rev.* **1997**, *97* (3), 597−636.
(36) Schottel, B. L.; Chifotides, H. T.; Dumbar, K. R. Anion-π interactions. *Chem. Soc. Rev.* **2008**, *37* (1), 68−83.
(37) Lucas, X.; Bauzá, A.; Frontera, A.; Quinonero, D. A thorough anion−π interaction study in biomolecules: on the importance of cooperativity effects. *Chem. Sci.* **2016**, *7* (2), 1038−1050.
(38) *CrysAlisPro, ver. 1.171.38.46*; Rigaku Oxford Diffraction: Yarnton, U.K., 2018.
(39) Sheldrick, G. M. *SHELXT* − Integrated space-group and crystalstructure determination. *Acta Crystallogr., Sect. A: Found. Adv.* **2015**, *A71*, 3−8.
(40) Sheldrick, G. M. Crystal structure refinement with SHELXL. *Acta Crystallogr., Sect. C: Struct. Chem.* **2015**, *C71*, 3−8.
(41) Dolomanov, O. V.; Bourhis, L. J.; Gildea, R. J.; Howard, J. A. K.; Puschmann, H. *OLEX2*: a complete structure solution, refinement and analysis program. *J. Appl. Crystallogr.* **2009**, *42*, 339−341.

https://dx.doi.org/10.1021/acs.inorgchem.9b03664
Inorg. Chem. 2020, 59, 3993−4001